RESEARCH ARTICLE

ISRS

Visible-Near Infrared Reflectance Spectroscopy for Rapid Characterization of Salt-Affected Soil in the Indo-Gangetic Plains of Haryana, India

Rajeev Srivastava[1] · Madhurama Sethi[2] · R. K. Yadav[2] · D. S. Bundela[2] ·
Manjeet Singh[3] · S. Chattaraj[1] · S. K. Singh[1] · R. A. Nasre[1] · Sita Ram Bishnoi[2] ·
Sanjay Dhale[1] · D. S. Mohekar[1] · A. K. Barthwal[1]

Abstract Management of salt-affected soils is a challenging task in the input intensive rice-wheat cropping zone of the Indo-Gangetic plains (IGP). Timely detection of salt-affected areas and assessment of the degree of severity are vital in order to narrow down the potential gap in yield. Conventional laboratory techniques of saturation extract electrical conductivity (EC_e) and sodium adsorption ration (SAR) for soil salinity assessment are time-consuming and labour intensive; the VNIR (visible-near infrared) reflectance spectroscopy technique provides ample information on salinity and its attributes in an efficient and cost-effective way. This study aims to develop robust soil reflectance spectral models for rapid assessment of soil salinity in the salt affected areas of the IGP region of Haryana using VNIR reflectance spectroscopy. The results indicated that the spectral region between 1390 and 2400 nm was highly sensitive to measure changes in salinity. The developed hyperspectral models explained more than 80 % variability in EC_e, and other salinity related attributes (saturated extract Na^+, $Ca^{2+} + Mg^{2+}$, Cl^- and SAR) in the validation datasets. With the increasing availability of data from hyperspectral sensors in near future, the study will be very useful in real time monitoring of soils in the spatio-temporal context; enabling the farmers of IGP area to deal with salt degradation more effectively and efficiently.

✉ Rajeev Srivastava
rajeev.nbss@gmail.com

[1] National Bureau of Soil Survey and Land Use Planning (ICAR), Amravati Road, Nagpur 440 033, Maharashtra, India

[2] Central Soil Salinity Research Institute, Karnal 132 001, India

[3] Punjab Agricultural University, Ludhiana 141 004, India

Introduction

Salt-affected soils in India, generally, occur in the arid and semiarid regions and canal command areas. Agricultural input intensification in areas with shallow ground water table depth has accelerated salt accumulation and compounded the problem further, eventually leading to yield reduction, particularly in the major food growing regions of the Indo-Gangetic plains (IGP). Management of salt-affected soils in the IGP is influenced by the variability in salinity/alkalinity levels. Therefore, timely detection of salt-affected areas, assessment of its extent and degree of severity are essential to narrow down the potential yield gap in this "yield fatigue" region under rice-wheat cropping system.

Mapping of salt-affected soils based on conventional methods demands a great deal of time and capital. Further, the laboratory techniques used for characterizing the attributes of salt-affected soils are time-consuming and costly. On the contrary, the remote sensing techniques are quick, real-time and cost effective for mapping and monitoring soil salinity in a larger coverage at regular intervals. Diffuse reflectance spectroscopy (DRS) which is a non-destructive method has been widely tested for characterization of various attributes of soils (Ben-Dor and Banin 1995; Shepherd and Walsh 2002; Srivastava et al. 2004, 2015; Brown et al. 2006; Viscarra Rossel et al. 2006; Summers et al. 2011). The advantages of DRS are its simplicity of sample preparation (sieving of soils), no use of chemical reagents, non-destructive nature, apart from speed, economy and precision. Further, the laboratory

Springer

measured hyperspectral reflectance data in a narrow (1 nm) band width in the visible-near infrared (VNIR) region (~400 to 2500 nm) provide ample information for distinguishing salt minerals as most of their characteristic absorption features occur in this region (Crowley 1991; Drake 1995; Ben-Dor et al. 2002). A fair amount of research has been directed towards the identification of diagnostic absorption bands in the spectrum of evaporite minerals and salt crust in both the field and the laboratory (Crowley 1991; Howari et al. 2002; Farifteh et al. 2006). This information is basically used to establish a statistical relationship between spectral properties of salt-affected soils and the presence or abundance of salt minerals in soil (Farifteh et al. 2004). Salt affected soils contain various proportions of cations (Na^+, Ca^{2+}, Mg^{2+}, K^+) and anions (Cl^-, SO_4^{2-}, CO_3^{2-}, HCO_3^-) that lead to different degrees of salinity as frequently indicated through electrical conductivity of saturated soil extract (EC_e) (Richards 1954). The minerals mainly responsible for soil salinity are carbonates, halides, sulfates, and borates. A noteworthy review of spectral characteristics of saline soils were made by Farifteh et al. (2006) and Metternicht and Zinck (2008). Unlike multiple linear regression and principal component analysis, the partial least square regression (PLSR) approach is able to model number of response variables simultaneously while effectively dealing with strongly collinear and noisy independent variables (Wold et al. 2001; Brown et al. 2006). The PLSR technique has inferential capability, which can be modeled through a possible linear relationship between salt concentrations in soils and measured reflectance spectra; and also reported to yield equally good results in comparison to the complex ANN procedure (Farifteh et al. 2007).

However, these statistical relations of salt content with the spectrum is region specific, hence, breakthrough in discrimination of different degree of salinization can be possible if the spectral characteristics of saline soils and the underlying factors are examined based on locally developed hyperspectral models. The attempt has been made in the present investigation to develop the robust soil reflectance spectral models for rapid prediction of soil salinity in the salt-affected areas of the Indo-Gangetic Plains of Haryana, India using laboratory measured soil reflectance spectral data.

Material and Methods

Study Area

The soil samples for the present study were collected from the farmers' fields of three villages viz. Jagsi, Sonipat district (76° 38′ 52.45″ E, 29° 14′ 40.53″ N), Kahni, Rohtak district (76° 40′ 40.29″ E, 29° 0′ 29.51″ N) and Waiser, Panipat district

(76° 48′ 59.9″ E, 29° 22′ 0.78″ N) of the Haryana state representing varying soil salinity levels of the IGP (Fig. 1). Salient soil-site characteristics as observed through 2009 and 2010 in all the three villages are presented in Table 1. All the three sites had medium textured soil and are mostly under rice-wheat cropping system. Relatively high soil ECe values during May-June (Summer season) in surface layers of all the three sites might be due to upward movement of saline groundwater through capillary rise leading to salt deposition on evaporation (Verma et al. 1994).

The soils of Jagsi village, initially, had moderate to high salinity hazards and poor soil physical properties. However, with the installation of subsurface drainage system in the year 2009, these soils were reclaimed and brought under cultivation. Kahni village represented extremely degraded salt-affected soils dominantly covered with salt encrustation. The soils of Waiser village were mainly saline-sodic in nature. The application of gypsum in soil has improved the soil condition for raising fairly good crop during the rice and wheat cropping cycle. Thus, all the three selected sites represented varying degree of salinity/sodicity levels for soil sampling to develop a robust hyperspectral model for soil salinity/sodicity assessment in the IGP.

Soil Sampling and Soil Analysis

Surface soil samples (0–1 cm and 0–15 cm) were collected from these three villages during 2009 to 2010 just after the harvest of rice and wheat crops. The soil samples from 0–1 cm depth were collected by scrapping after removing surface plant/grass debris and salt- efflorescence, if any. The sampling from 0–1 cm depth was done because it might contain relatively higher concentration of salt as compared to composite samples of 0–15 cm, and hence, more variability in salt content in the samples for statistical analysis. A total of 806 samples were collected, air-dried, ground and passed through a 2 mm sieve. Soil properties that are known to be affected by accumulation of salts and/ or influencing soil optical properties were analyzed following standard laboratory techniques (Van Reeuwijk 1993). Soil electrical conductivity (EC_e) and pHs (saturation extract pH) were measured in the saturated soil extract. Exchangeable cations Ca^{2+} + Mg^{2+} (Cheng Kuang and Bray 1951), Na^+, K^+ and anions CO_3^{2-}, HCO_3^-, Cl^- (Richards 1954) and SO_4^{2-} (Chesnin and Yien 1951) were determined in the saturation extract.

Hyperspectral Reflectance Data Acquisition

Diffuse reflectance spectra of each air-dried soil sample (<2 mm size) were acquired in a laboratory setting (Srivastava et al. 2015) using a ASD FieldSpec Pro FR spectroradiometer device. The device covers visible to near-

Fig. 1 Location of the study area

infrared wavelength range (350 to 2500 nm). Samples were illuminated from above with two tungsten quartz halogen filament lamps in housings with aluminum reflectors (Lowel pro-lamp, Lowel-Light Manufacturer Inc., New York, NY) with 50 W bulb; 3200 K colour temperature (WelchAllyn, Skaneateles Falls, NY). Reflected light was collected with a 25° field-of-view foreoptic that was kept vertically at a distance of 5 cm above the sample. Reflectance was calibrated against white Spectralon panel (Labsphere, Sutton, NH). Reflectance readings for each wavelength band were expressed relative to the spectralon readings. Variation in overall spectral shape among soil samples were studied by plotting the relative reflectance values against different wavebands.

Data Processing and Transformation

The original spectra consisting of relative reflectance values of 2151 points (at 1 nm interval) between 350 and 2500 nm were weighted averaged at every tenth-nanometer wavelength interval by integration technique as described by Srivastava

et al. (2015). The integrated value of soil reflectance at every tenth nanometer wavelength (360, 370,…..2490 nm) was determined by Eq. (1):

$$IR = \frac{\sum_i^n wi.ri}{\sum_i^n wi} \tag{1}$$

Where, IR=Integrated reflectance at every tenth-nanometer interval, wi = wavelength at 1 nm interval between 350–2500 nm, ri = reflectance value at wi wavelength

For example, the new reflectance value for 360 nm represented an integrated value of the original reflectance values from 356 to 365 nm. Similarly, the reflectance at 700 nm was an integrated reflectance values from 696 to 705 nm. This procedure resulted in a new dataset, with reflectance values specified for 214 wavelengths for all samples.

The integrated spectral data were then subjected to Savitzky-Golay (Savitzky and Golay 1964) first derivative

Table 1 Timeline soil-site characteristics of three villages under study

Location	Year	Total annual rainfall (mm)	Soil sampling month	Sampling depth (cm)	No. of samples	pHs	ECe (mSm^{-1})	Soil type	Cropping sequence
Jagsi, Sonipat district, Haryana	2009	582.8	Oct-Nov	0–1	66	7.8–8.8	220–2520	Sandy loam, loam to clay loam	Rice /Wheat
				0–15	67	8.1–8.8	97–1010		
	2010	766.4	May-June	0–1	73	7.4–8.5	240–4300		
				0–15	75	7.4–8.7	140–2700		
Kahni, Rohtak district, Haryana	2009	404.1	Oct-Nov	0–1	64	7.0–9.0	380–16720	Loam to silty loam	Rice/Bajra/Wheat
				0–15	65	7.7–9.0	100–13000		
	2010	486.0	May-June	0–1	62	7.2–9.0	200–17700		
				0–15	72	7.8–9.1	130–12000		
Waiser, Panipat district, Haryana	2009	272.0	Oct-Nov	0–1	57	7.2–8.3	60–750	Loam to clay loam	Rice/Wheat
				0–15	61	7.3–9.1	40–250		
	2010	505.1	May-June	0–1	65	6.9–8.3	100–430		
				0–15	79	7.0–9.1	60–370		

transformation in Unscrambler 10.1 (CAMO Software AS, Oslo, Norway) software.

Statistical Modelling

The soil samples collected from three villages were combined with the aim of producing a more robust hyperspectral model for soil salinity measurement; since pooling represent a higher diversity of soil characteristics with a range of salinity level. The whole dataset ($n = 806$) was randomly divided into two subsets viz. calibration and validation datasets. The Levene's test ($p = 0.402$) for equality of variances (Levene 1960) and the Student's 't' test ($p = 0.97$) for equality of means in ECe values between calibration and validation sets indicate that validation datasets are truly representative. Calibrations between soil reflectance and soil parameters were performed in Unscrambler-V.10.1 software using partial least square regression (PLSR) technique. The best model was chosen based on coefficient of determination of validation (r^2, equation (2)), root mean square error of prediction (RMSEP; Eq. (2)) and ratio of performance to deviation (RPD, Eq. (4)).

$$r^2 = 1 - \left(\frac{\sum_{i}^{n} (Y_{pred} - Y_{meas})^2}{\sum_{i}^{n} (Y_i - Y_{mean})^2} \right) \quad (2)$$

$$\text{RMSEP} = \sqrt{\frac{\sum_{i}^{n} (Y_{pred} - Y_{meas})^2}{n-1}} \quad (3)$$

$$\text{RPD} = SD_{val.} / \text{RMSEP} \quad (4)$$

where: Y_{pred} = predicted values; Y_{mean} = mean of measured values; Y_{meas} = measured values; n = number of predicted/measured values with i = 1,2,...... n; $SD_{val.}$ = standard deviation

of measured values in the validation set; and RMSEP = root mean square error of prediction of validation dataset.

Predictive performance of the developed PLSR hyperspectral models for ECe and SAR was evaluated following diagnostic screening test (Shepherd and Walsh 2002) based on a threshold value to classify soil samples either as normal *or* abnormal. The objective was to assess how successful the model is in discriminating normal and abnormal samples. The threshold values used for differentiating normal and abnormal samples for ECe and SAR were 400 mSm^{-1} and 13, respectively. The two parameters, namely *Specificity* (percentage of normal cases correctly predicted with respect to threshold value), and *Sensitivity* (percentage of abnormal cases correctly predicted with respect to threshold value) were used in defining the predictive performance.

Results and Discussion

Chemical Composition of Salt-Affected Soils

The statistical parameters of the soil chemical properties of the processed soil samples studied under laboratory conditions are given in Table 2. The data indicate that soil pHs varies between 6.9 and 9.1 and majority of the samples (over 75 %) have soil pHs less than 8.5. The ECe values vary from 40 to 17700 mSm^{-1} (millisiemens/meter) and nearly half of the samples have ECe values of 450 mSm^{-1}. This indicates that majority of the soils in study area are saline rather than saline-sodic (only one fourth of the total samples are having pH in sodic range). Among the cations, average Na$^+$ concentration (135.7 meq l^{-1}) was the highest followed by Ca^{2+} + Mg^{2+} (43.8 meq l^{-1}); whereas amongst the anions, Cl$^-$ and SO$_4^{2-}$ (122.7 and 45.3 meq l^{-1}, respectively) dominated over the carbonate and bi-carbonate

Table 2 Descriptive statistical parameters of soil chemical properties

Soil property	N	Min	Max	Mean	SD	Percentile		
						25th	50th	75th
pH_s	805	6.9	9.1	8.1	0.4	7.9	8.2	8.4
EC_e (mS m^{-1})	806	40	17700	1297	2350	160	450	1180
$CaCO_3$ (g kg^{-1})	806	1.0	130.0	16.0	13.5	8.0	12.5	20.0
SE Na^+ (meq l^{-1})	806	1.9	2120.0	135.7	242.3	11.2	50.0	125.0
SE K^+ (meq l^{-1})	806	0.03	159.0	2.6	11.8	0.2	0.4	0.9
SE $Ca^{2+} + Mg^{2+}$ (meq l^{-1})	805	1.5	652.0	43.8	71.7	10.0	17.5	48.0
SE CO_3^{2-} (meq l^{-1})	806	0	8.0	0.8	1.3	0.0	0.0	1.0
SE HCO_3^- (meq l^{-1})	806	0	63.2	5.6	5.1	3.0	4.3	7.0
SE Cl^- (meq l^{-1})	806	2.0	2110.0	122.7	265.2	8.0	25.8	92.3
SE SO_4^{2-} (meq l^{-1})	796	0.3	524.0	45.3	65.4	6.7	26.1	48.3
SAR ([meq l^{-1}]$^{0.5}$)	805	0.72	574.6	23.9	31.9	5.3	16.3	29.1

SE saturation extract

anions in the soils. The soils, in general, are calcareous in nature (mean $CaCO_3$ concentration = 16.0 g kg^{-1}).

Soil Spectral Characteristics and its Correlation with Soil Properties

The reflectance spectra and their first derivatives between 350 and 2500 nm wavelength for all the soil samples (<2 mm size) under study are shown in Fig. 2a, b. The reflectance spectra showed prominent absorption features around 1400, 1900 and 2200 nm. Similar to reflectance spectra, the 1st derivative transformation data also yielded the diagnostic absorption features (the magnitude of which was more pronounced around 1900 nm followed by 1400 and 2200 nm); all of which are known to be related to features of free water (~1400 and ~1900 nm) and clay lattice OH features (~1400 and ~2200 nm) (Hunt 1982). Hence, these absorption bands could be more responsive towards the presence of salt minerals in the salt affected soils; the sensitivity of which will depend upon the nature and amount of the hygroscopic minerals

present in the soil samples. The mean representative spectra of total 359 non-saline (< 400 mSm^{-1}), 179 slightly saline (400–800 mSm^{-1}), 106 moderately saline (800–1600 mSm^{-1}), 107 strongly saline (1600–5000 mSm^{-1}) and 55 very strongly saline (>5000 mSm^{-1}) soils (Fig. 3) of the study area revealed the fact that the intensity of absorption peaks near 1900 nm region wavelengths shift towards the higher wavelength with the increase in soil salinity.

The statistical correlation of soil chemical properties with first derivative soil reflectance data showed both positive and negative correlations at various wavelengths across the spectrum (Fig. 4). Further, ECe (electrical conductivity of saturation extract), saturated extract Na^+, $Ca^{2+} + Mg^{2+}$, Cl^- and SO_4^{2-} showed similar pattern of correlation at different wavelengths with 1st derivative soil reflectance values. Relatively high correlation of ECe, saturated extract Na^+, $Ca^{2+} + Mg^{2+}$, Cl^- and SO_4^{2-} with first derivative soil reflectance values was observed between 1400 and 2400 nm which indicates that this region is highly sensitive to change in salinity levels. Farifteh et al. (2008) also reported an increase in soil salinity induced
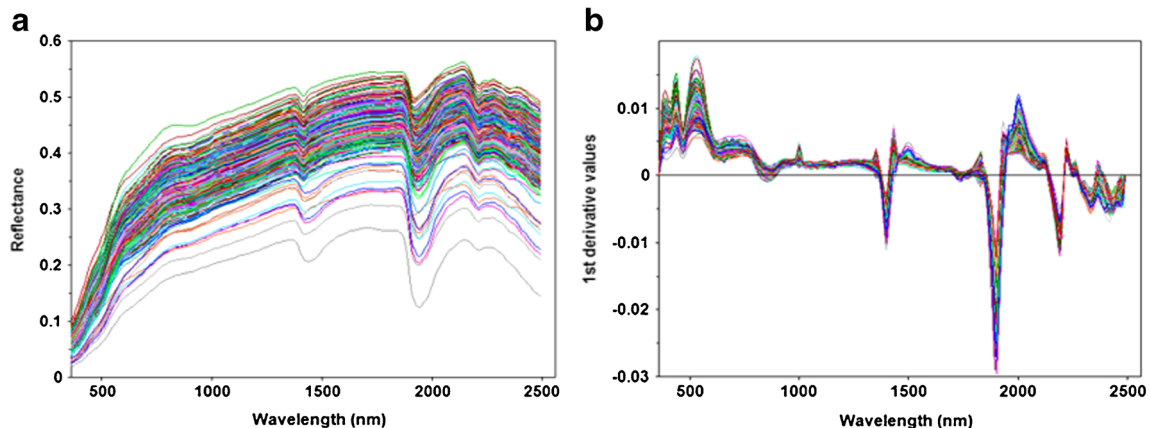

Fig. 2 Reflectance spectra (**a**) and first derivative equivalents (**b**) for all salt affected soils under study
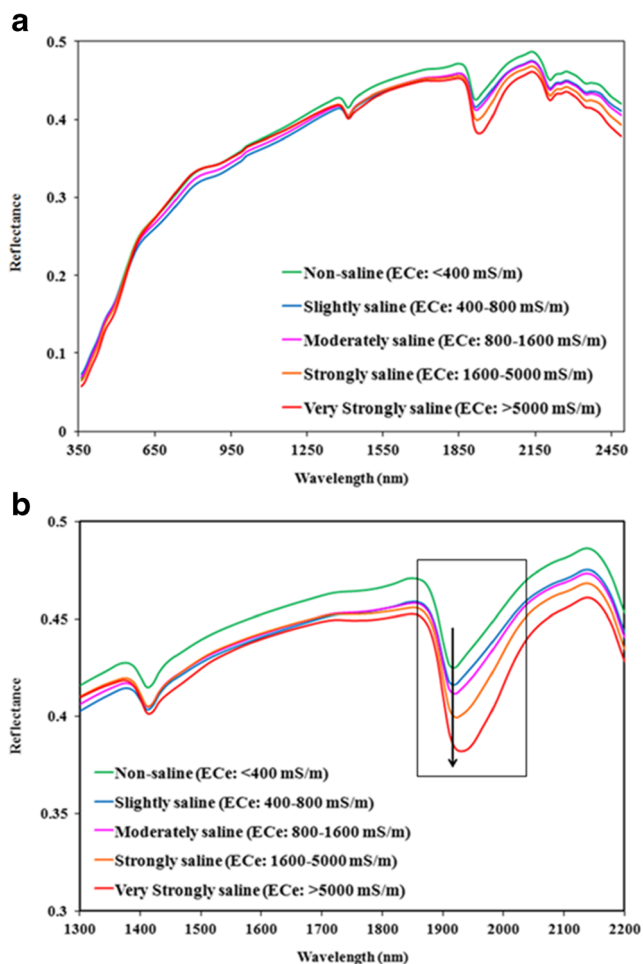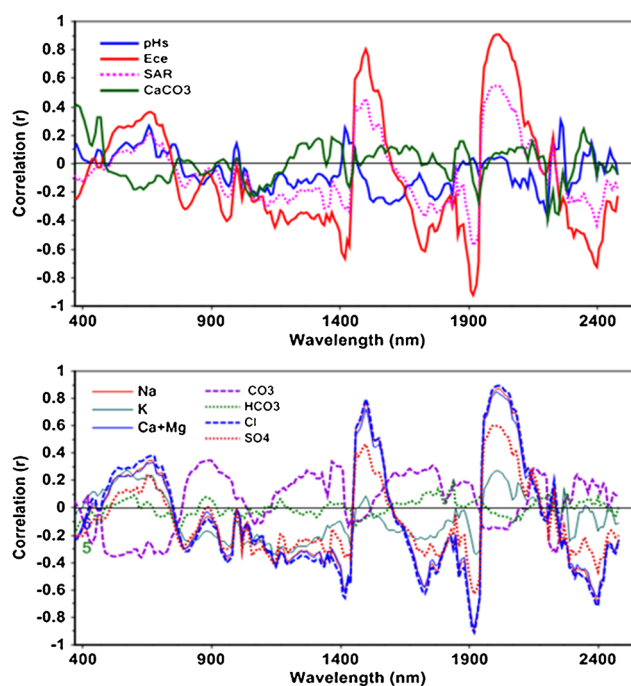
Fig. 4 Correlation of different soil salinity parameters with 1st derivative soil reflectance between 400 and 2450 nm region

Partial Least Square Regression (PLSR) Modeling of Hyperspectral Data

Calibration

Salt-affected soil properties viz., pHs, cations (Na^+ and Ca^{2+} + Mg^{2+}), anions (Cl^- and SO_4^{2-}, CO_3^{2-} and HCO_3^-) and SAR (sodium adsorption ratio) were calibrated against the 1st derivative reflectance wavebands between 1400 and 2450 nm region (Table 3). Very good calibrations were obtained for ECe ($r^2 = 0.94$, RMSE= 5.86), Ca^{2+} + Mg^{2+} ($r^2 = 0.89$, RMSE= 1.23), Na^+ ($r^2 = 0.91$, RMSE= 2.29), Cl^- ($r^2 = 0.93$, RMSE= 2.19), SO_4^{2-} ($r^2 = 0.76$, RMSE= 1.69) and SAR

Fig. 3 Mean representative spectra of soils with different salinity levels as indicated by the range of ECe in mSm^{-1} between 350 and 2500 nm region (**a**) and depicting shift in absorption peak towards higher wavelength due to increase in salinity (**b**)

changes in soil reflectance for wavebands higher than 1300 nm, particularly in the water absorption bands (around 1400 and 1900 nm).

Table 3 Summary statistics for the spectral models developed by partial least-square regression (PLSR)

S. No.	Soil parameters*	No. of factors	Calibration set			Validation set				
			N	r^2	RMSE	N	SD*	r^2	RMSEP	RPD
1	pH (SE)	6	402	0.39	0.30	403	0.37	0.45	0.27	1.38
2	ECe (SE; mS m^{-1})	4	403	0.93	6.00	403	22.5	0.94	5.64	3.98
3	SE Ca^{2+} +Mg^{2+} (meq l^{-1})	3	402	0.85	1.49	403	3.57	0.83	1.46	2.44
4	SE Na$^+$ (meq l^{-1})	5	403	0.89	2.38	403	7.55	0.86	2.81	2.69
5	SE Cl$^-$ (meq l^{-1})	3	403	0.92	2.18	403	7.70	0.90	2.39	3.22
6	SE SO$_4^{2-}$ (meq l^{-1})	5	398	0.63	2.30	398	3.72	0.68	2.11	1.76
7	SE CO$_3^{2-}$ (meq l^{-1})	6	403	0.23	0.62	403	0.72	0.31	0.60	1.20
8	SE HCO$_3^-$ (meq l^{-1})	6	400	0.15	0.67	403	0.80	0.12	0.73	1.09
9	SAR ([meq l^{-1}]$^{0.5}$)	7	398	0.75	1.08	398	2.5	0.80	0.95	2.65

*Square root transformation was applied on all soil parameters except pHs (no transformation)

(r^2 = 0.76, RMSE= 1.04). Higher regression coefficients (r^2) were achieved for all the PLSR models developed for predicting soil salinity parameters (except pHs, carbonate and bicarbonate anions) in the calibration sets by removing very few outliers as indicated by N (Table 3). The poor calibration of PLSR models for pHs, CO_3^{2-} and HCO_3^{-} may be due to narrow variations in soil samples as compared to the other soil parameters.

Validation

The predictive performances of the PLSR models for different salinity variables were evaluated based on r^2, RMSE and RPD indices obtained in the independent validation set. The r^2 indicates the percentage of the variation in the dependent variable that is accounted for by the independent variables.

The RMSEP estimates the variation of predicted values around observed values, and as this approaches to zero, prediction performance of the equation increases. The RPD is the factor, by which the prediction accuracy has been increased compared to using the mean composition for all samples. Chang et al. (2001) grouped the prediction quality of soil properties using VNIR spectroscopy into three categories based on RPD values in the ranges of >2.0, 1.4–2.0, and <1.4 to indicate excellent, acceptable and poor predictions, respectively. They suggested that the predictions in the middle category could be improved using different calibration strategies, but the properties in the poor category may not be reliably predicted using reflectance spectroscopy.

The application of developed calibration models to soil attributes also resulted in high r^2 and low RMSE for all the attributes except soil pHs, CO_3^{2-} and HCO_3^{-} in the
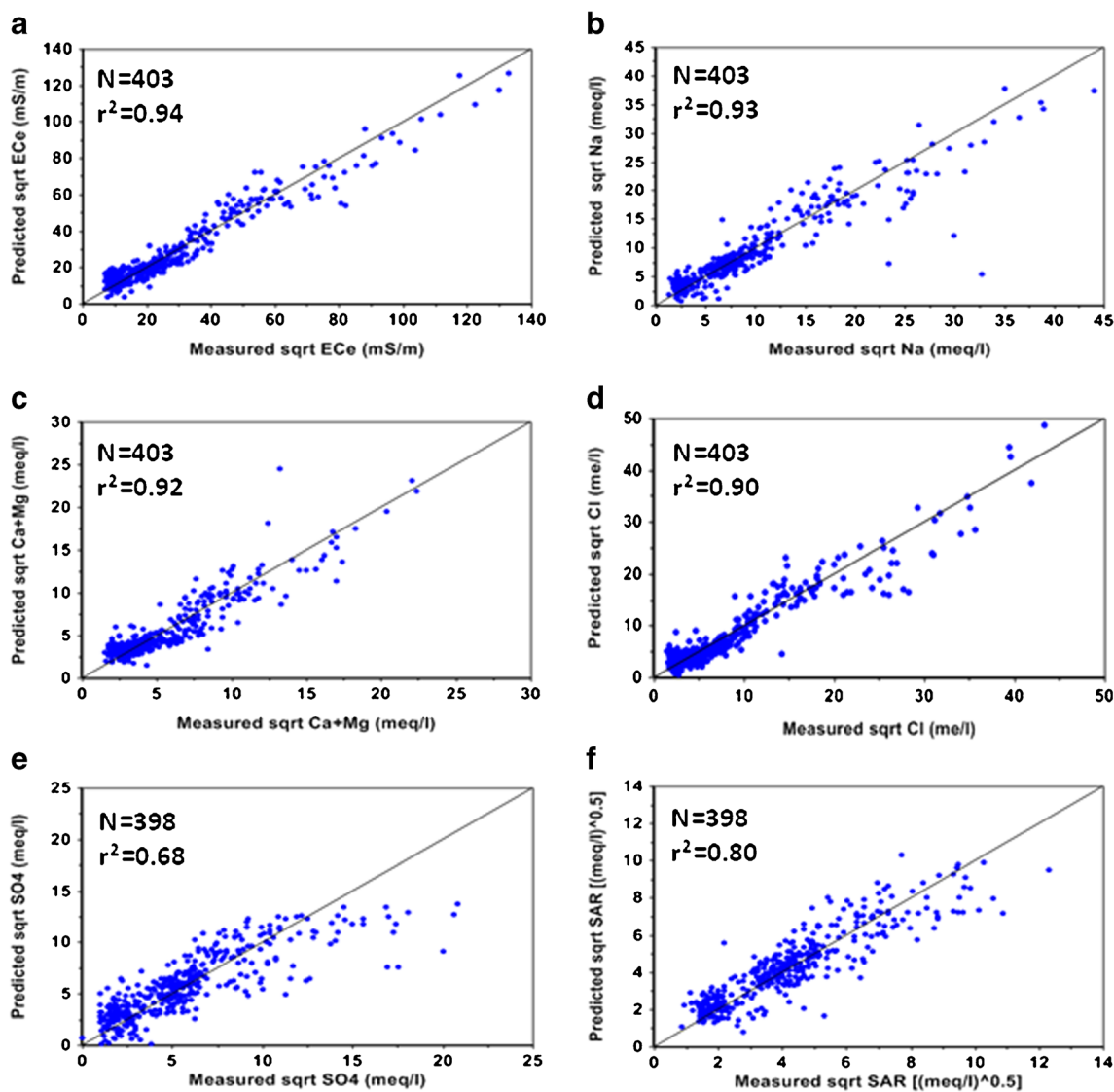

Fig. 5 Scatter plot of measured and predicted values (in square root transformation) of saturation extract (**a**) ECe (**b**) Na$^+$ (**c**) Ca^{2+}+Mg^{2+} (**d**) Cl$^-$ (**e**) SO$_4^{2-}$ and (**f**) SAR in validation datasets

independent validation datasets (Table 3). The calibration models obtained for soil pHs ($r^2 = 0.57$), CO_3^{2-} ($r^2 = 0.28$) and HCO_3^- ($r^2 = 0.35$) did not show good prediction due to low variability in the datasets. The high RPD values (> 2.0) obtained for ECe, SAR, Na^+, $Ca^{2+} + Mg^{2+}$ and Cl^- indicate that these properties can be reliably predicted from the spectral models (Fig. 5) whereas the spectral model of SO_4^{2-} (RPD = 1.76) needs further improvement with larger datasets. Relatively greater variability in prediction at higher concentrations than lower concentrations of different soil salinity variables (Fig. 5) may be because of error in the laboratory analytical methods rather than genuine lack of prediction power of the spectral models. Shepherd and Walsh (2002) observed that increased analytical error at higher concentrations could be expected because of greater variability in amounts of ion extracted and the need for increasing number of dilutions.

Figure 6 depicts the regression coefficients of PLSR models for ECe and SAR. Relatively higher absolute values of regression coefficients at wavebands 1810, 1930, 1990 and 2210 nm for ECe and 1420, 1890, 1940 and 2360 nm for SAR indicated that these wavebands are contributing significantly in prediction of these soil salinity variables. The predictive performance of ECe model in the validation dataset (Table 4) yielded satisfactory discrimination between saline and non-saline soil samples (critical limit for ECe= 400 mSm^{-1}) as the specificity and sensitivity indices obtained were 94 and 82 %, respectively. Similar predictive performance with high specificity (84 %) and sensitivity (92 %)
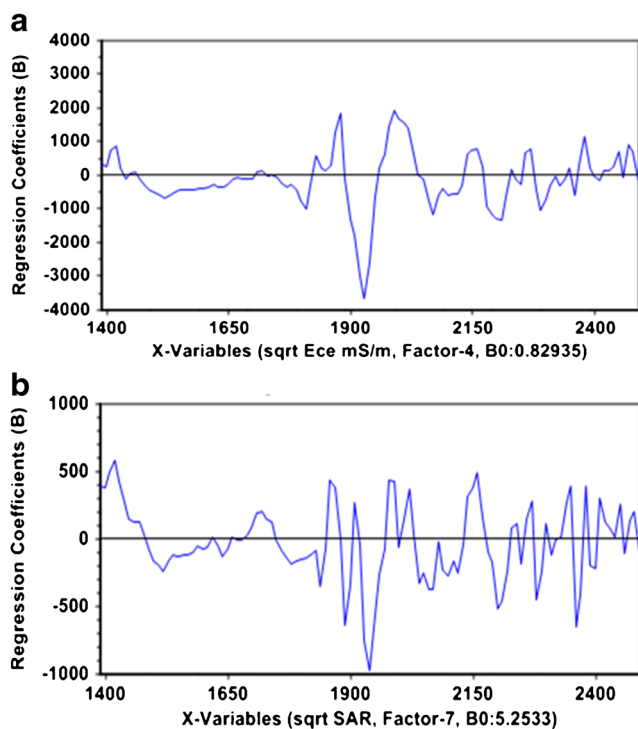
Table 4 Predictive performance of validation dataset

Salinity class	Threshold	Specificity	Sensitivity	N_{nor}	N_{abn}
EC_e (mSm^{-1})	<400	94	82	179	224
SAR ($[meq\ l^{-1}]^{0.5}$)	<13	84	92	164	235

N_{nor} no. of normal cases in validation samples, N_{abn} no. of abnormal cases in validation samples

indices was also obtained in case of SAR model for discriminating sodic and non-sodic soils (critical limit for SAR= 13).

The study indicate that ECe, being the most commonly used indicator for measuring the degree of soil salinity, can be effectively retrieved or predicted through laboratory based hyperspectral model. In addition to ECe, other salinity related parameters namely saturated extract cations (Na^+ and $Ca^{2+} + Mg^{2+}$), selective anions (Cl^- and SO_4^{2-}) and SAR might also be estimated through the hyperspectral models with reasonably good accuracy in the study area. However, all throughout our discussion we have not detailed the results regarding estimation of saturation extract pHs (which is also an important indicator of soil salinity) as because the findings under the study area were not encouraging. The poor prediction for pHs in this study could be attributed to its narrow range, as with Viscarra Rossel et al. (2006). But at the same time, this might not be considered as a limitation of hyperspectral models as all these spectral models are region specific in nature. In recent years continuum-removal (CR) analysis through fitting of a convex hull to isolate individual absorption features of interest are becoming popular (Farifteh et al. 2008). But, in our study we had acquired a reasonably good accuracy without use of such transformation.

Conclusions

The potential of hyperspectral data and quantification of soil salinity and sodicity in VNIR range over the study area of IGP region was documented through this study. It can be concluded that the soil reflectance data between 1390 and 2400 nm region can be successfully used for rapid prediction of saline soils as well as the type of salt present in the soils of the IGP region. The hyperspectral models of ECe, SAR and other salinity related attributes developed with large number of dataset having broad range of salinity were able to capture more than 75 % of the variability. Keeping in view, the importance of this major rice-wheat cropping zone; the models developed might be used to characterize other salt affected soils occurring in this region subjected to optimum validation. With the availability of high resolution hyperspectral satellite data and growing interest of scientific community in precise characterization of natural resources; our findings on prediction of soil salinity and sodicity through hyperspectral models

Fig. 6 Partial least square regression coefficients for saturation extract ECe (**a**) and SAR (**b**) at different wavebands

are encouraging as it might assist in real time characterization and monitoring of salinity over the spatio-temporal context; enabling the farmers of IGP area to cope up with this degradation in a better way.

References

Ben-dor, E., & Banin, A. (1995). Near-infrared analysis as a rapid method to simultaneously evaluate several soil properties. *Soil Science Society of America Journal, 59*, 364–372.

Ben-Dor, E., Patkin, K., Banin, A., & Karnieli, A. (2002). Mapping of several soil properties using DAIS-7915 hyperspectral scanner data - a case study over clayey soils in Israel. *International Journal of Remote Sensing, 23*(6), 1043–1062.

Brown, D. J., Shepherd, K. D., Walsh, M. G., Dewayne Mays, M., & Reinsch, T. G. (2006). Global soil characterization with VNIR diffuse reflectance spectroscopy. *Geoderma, 132*(3–4), 273–290.

Chang, C. W., Laird, D. A., Mausbach, M. J., & Hurburgh, C. R. (2001). Near-infrared reflectance spectroscopy-principal components regression analyses of soil properties. *Soil Science Society of America Journal, 65*(2), 480–490.

Cheng Kuang, L. U., & Bray, R. H. (1951). Determination of calcium and magnesium in soil and plant material. *Soil Science, 72*(6), 449–458.

Chesnin, L., & Yien, C. H. (1951). Turbidimetric determination of available sulphates. *Soil Science Society of America Journal, 15*(c), 149–151.

Crowley, J. K. (1991). Visible and near-infrared (0.4–2.5 μm) reflectance spectra of playa evaporite minerals. *Journal of Geophysical Research, 96*(B10), 16231–16240.

Drake, N. A. (1995). Reflectance spectra of evaporite minerals (400–2500 nm): application for remote sensing. *International Journal of Remote Sensing, 16*(14), 2555–2571.

Farifteh, J., Bouma, A., & Van Der Meijde, M. (2004). *A new approach in the detection of salt affected soils; integrating surface and subsurface measurements.* Poster presented at "Near surface 2004", 10th EAGE European Meeting of Environmental and Engineering Geophysics, Utrecht, The Netherlands.

Farifteh, J., Farshad, A., & George, R. J. (2006). Assessing salt-affected soils using remote sensing, solute modelling, and geophysics. *Geoderma, 130*(3–4), 191–206.

Farifteh, J., Van Der Meer, F., Atzberger, C., & Carranza, E. J. M. (2007). Quantitative analysis of salt affected soil reflectance spectra: a comparison of two adaptive methods (PLSR and ANN). *Remote Sensing of Environment, 110*(1), 59–78.

Farifteh, J., Van Der Meer, F., Van Der Meijde, M., & Atzberger, C. (2008). Spectral characteristics of salt-affected soils: a laboratory experiment. *Geoderma, 145*(3–4), 196–206.

Howari, F. M., Goodell, P. C., & Miyamoto, S. (2002). Spectral properties of salt crusts formed on saline soils. *Journal of Environmental Quality, 31*(5), 1453–1461.

Hunt, G. R. (1982). Spectroscopic Properties of Rocks and Minerals. In: *Handbook of Physical Properties of Rocks.* Boca Raton, FL: CRC Press.

Levene, H. (1960). Robust tests for equality of variances. In: *Contributions to probability and statistics: Essays in honor of Harold Hotelling.* Stanford, California: Stanford University Press.

Metternicht, G., & Zinck, J. A. (2008). *Remote sensing of soil salinization: impact on land management.* Boca Raton: CRC Press.

Richards, L. A. (1954). *Diagnosis and improvement of saline and saline and alkali soils (agricultural handbook No* (60)). Washington, DC: US Department of Agriculture, US Government Printing Office.

Savitzky, A., & Golay, M. J. E. (1964). Smoothing and differentiation of data by simplified least squares procedure. *Analytical Chemistry, 36*(8), 1627–1639.

Shepherd, K. D., & Walsh, M. G. (2002). Development of reflectance spectral libraries for characterization of soil properties. *Soil Science Society of America Journal, 66*(3), 988–998.

Srivastava, R., Prasad, J., & Saxena, R. K. (2004). Spectral reflectance properties of some swell-shrink soils of Central India as influenced by soil properties. *Agropedology, 14*(1), 45–54.

Srivastava, R., Sarkar, D., Mukhopadhayay, S. S., Sood, A., Singh, M., Nasre, R. A., & Dhale, S. A. (2015). Development of hyperspectral model for rapid monitoring of soil organic carbon under precision farming in the indo-gangetic plains of Punjab, India. *Journal of the Indian Society of Remote Sensing, 43*(4), 751–759.

Summers, D., Lewis, M., Ostendorf, B., & Chittleborough, D. (2011). Visible near-infrared reflectance spectroscopy as a predictive indicator of soil properties. *Ecological Indicators, 11*, 123–131.

Van Reeuwijk, L. P. (1993). *Procedures for soil analysis. Technical paper No. 9.* Wangeningen: International Soil Reference and Information Centre (ISRIC).

Verma, K. S., Saxena, R. K., Barthwal, A. K., & Deshmukh, S. N. (1994). Remote sensing technique for mapping salt affected soils. *International Journal of Remote Sensing, 15*(9), 1901–1914.

Viscarra Rossel, R. A., Walvoort, D. J. J., Mcbratney, A. B., Janik, L. J., & Skjemstad, J. O. (2006). Visible, near infrared, mid infrared or combined diffuse reflectance spectroscopy for simultaneous assessment of various soil properties. *Geoderma, 131*(1–2), 59–75.

Wold, S., Sjöström, M., & Eriksson, L. (2001). PLS-regression: a basic tool of chemometrics. *Chemometrics and Intelligent Laboratory Systems, 58*(2), 109–130.